Electrical Characterization of Textile Transmission Lines

Didier Cottet, *Student Member, IEEE,* Janusz Grzyb, *Student Member, IEEE*, Tünde Kirstein, and Gerhard Tröster, *Senior Member, IEEE*

***Abstract*—In this paper, electrical characterization and modeling of conductive textiles are presented. A dedicated measurement setup has been developed to allow reliable connection of the textile samples with the equipment cables. Geometrical fabric structures and fabrication tolerances as well as high frequency properties up to 6 GHz for four types of textiles have been determined. Transmission lines with controlled characteristic impedance have been realized enabling the characterization of typical line attenuation factors. This work shows that textile transmission lines can be used for frequencies up to 1.2 GHz and 120 MHz with the maximal lengths of 10 and 100 cm, respectively.**

***Index Terms*—Attenuation constants, characteristic impedance, conductive textiles, transmission lines, wearable computing.**

I. Introduction

THE VISION behind wearable computing sketches future electronic systems to be an integral part of our everyday outfit. Such electronic devices have to meet special requirements concerning wearability. Design guidelines for wearable systems are described in [1]. Some approaches have been made to embed electronic components into clothing [2]–[4]. These garments contain conventional cables, miniaturized electronic components and special connectors. As humans prefer to wear comfortable textiles rather than hard, rigid boxes, first efforts have been made to use the textiles themselves for electronic functions [5]–[7]. An overview of smart fibers, fabrics and clothing is given in [8].

Our approach uses conductive textiles for signal transmission. In this way conventional wires and even whole circuit boards could be replaced by textile fabrics. We carried out systematic investigations of the electrical performance of conductive textiles. High frequency wires are not only characterized by their resistance but by transmission and wave effects. These effects are influenced by the line geometries and the surrounding material. That means that apart from the conductive material also the geometrical structures that are created in the textile fabrication processes have to be considered.

II. Conductive Textiles

Some textile products with electrical properties have already been developed e.g., in the field of EMI shielding, static dissipation and resistive heaters. There are, however, some general difficulties in creating conductive textiles for clothing. Textiles used for clothing have to be flexible and elastic in order to achieve a high comfort of wearing. Fabrics need to have a low resistance to bending and shearing so that they can be easily deformed and draped. The more the clothes are tight the more they have to be flexible. For this reason fibers that are used should be fine ($< 1\ \mathrm{g/km}$) and fabrics should have a low weight per unit area (ca. 150 $\mathrm{g/m^2}$, usually not more than 300 $\mathrm{g/m^2}$). These demands are inconsistent with the materials and geometries that are needed for an electrical conductivity. Metal, carbon and conductive polymers are quite rigid and brittle materials. Nevertheless textile technologies have been developed to manufacture processable fibers and yarns out of these materials [9]. Methods of creating conductive threads are:

1) filling of fibers with carbon or metal particles;
2) coating of fibers with conductive polymers or metal;
3) use of continuous or short fibers that are completely made of conductive material.

Clothing fabrics have been manufactured out of these yarns which are comfortable enough and have a surface conductivity suitable for EMI shielding and static dissipation. However, data transmission require separate conductor lines. Fine metal threads (with diameters from 10–60 $\mu\mathrm{m}$) suit this purpose best because they provide a high conductivity as well as an acceptable textile characteristic. An important aspect is the possibility to apply insulating coatings on these fibers. These insulated fibers are able to withstand textile typical handling as for example washing and wrinkling without a damage of the insulation. The combination of such metal fibers with synthetic fibers leads to processable yarns that can be woven or knitted.

III. Textile Specifications

The examined fabrics contain polyester (PES) yarns that are twisted with one copper (Cu) thread. The copper threads have a diameter of 40 $\mu\mathrm{m}$ and are insulated with a polyesterimide coating. We used woven fabrics with a plain weave in our experiments because this construction represents the most elementary and simple textile structure. In addition to that such kind of material can provide a tight mesh of individually addressable wires that can be used for basic transmission lines as well as whole circuits. PES yarns with two different fineness ($167\cdot10^{-4}\ \mathrm{g/m}$ resp. $334\cdot10^{-4}\ \mathrm{g/m}$) have been used to create six different fabric types (Table I). All fabrics show a density of about 20 $\mathrm{cm/cm^2}$ in both directions, but the density is different according to the used PES yarn fineness. Two of the fabrics have copper threads in both directions (XY-direction), two

Manuscript received November 13, 2002; revised March 24, 2003.

The authors are with the Electronics Laboratory and the Wearable Computing Laboratory, Department of Information Technology and Electrical Engineering, ETH Zürich, Zürich 8092, Switzerland (e-mail: cottet@ife.ee.ethz.ch).

Digital Object Identifier 10.1109/TADVP.2003.817329

TABLE I
TEXTILES USED IN EXPERIMENTS

Yarn types	Woven fabric types
Yarn A: PES yarn $167{\cdot}10^{-4}$ g/m + Cu thread	*Fabric 1*: low density with Cu in both directions (XY)
Yarn B: PES yarn $167{\cdot}10^{-4}$ g/m	*Fabric 2*: low density with Cu in one direction (X)
	Fabric 3: low density without Cu
Yarn C: PES yarn $334{\cdot}10^{-4}$ g/m + Cu thread	*Fabric 4*: high density with Cu in both directions (XY)
Yarn D: PES yarn $334{\cdot}10^{-4}$ g/m	*Fabric 5*: high density with Cu in one direction (X)
	Fabric 6: high density without Cu

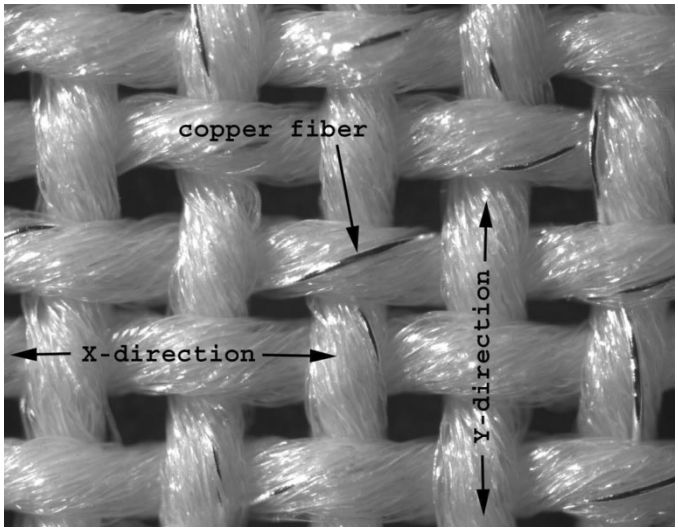

(a)

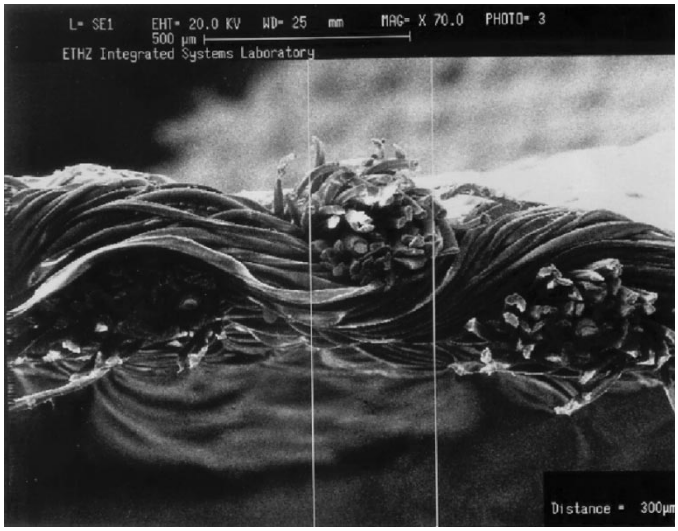

(b)

Fig. 1. (a) Woven fabric with metal fibers and (b) fabric cross section.

of them have copper threads just in X-direction and two of them are without copper. Fig. 1 shows fabric 4.

The geometry of textile materials is characterized by a complex hierarchical structure: bundles of fibers are twisted to create yarns, yarns are, e.g., woven to create fabrics. The fibers follow

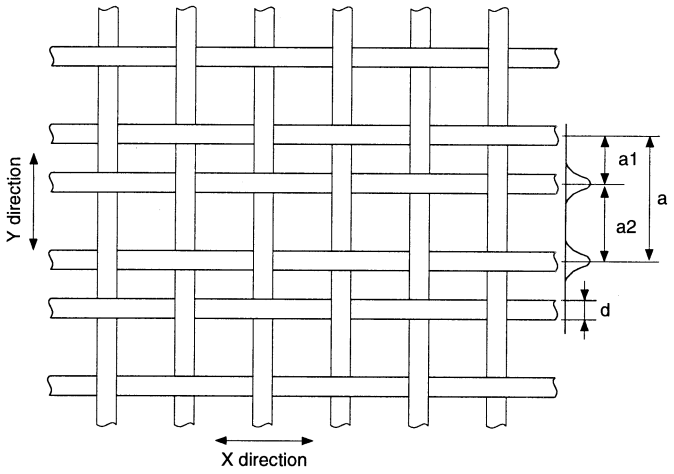

Fig. 2. Variations in textile geometry.

TABLE II
VARIATIONS OF TEXTILE GEOMETRIES USED IN THE EXPERIMENTS

Yarn types	Dimensions	Variations
PES yarn A, B	$a_1 = 411\mu$m	$\pm$ 7.3% ($\sigma = 30.0\mu$m)
	$a_2 = 481\mu$m	$\pm$ 6.7% ($\sigma = 32.2\mu$m)
	$a = 891\mu$m	$\pm$ 3.7% ($\sigma = 32.9\mu$m)
	$d = 228\mu$m	$\pm$ 11.1% ($\sigma = 25.3\mu$m)
PES yarn C, D	$a_1 = 356\mu$m	$\pm$ 6.8% ($\sigma = 24.0\mu$m)
	$a_2 = 519\mu$m	$\pm$ 4.4% ($\sigma = 22.8\mu$m)
	$a = 876\mu$m	$\pm$ 2.9% ($\sigma = 25.0\mu$m)
	$d = 334\mu$m	$\pm$ 8.4% ($\sigma = 28.0\mu$m)

a helical path within the yarn. The helical path of the metal threads can be seen in Fig. 1(a). When the yarns are woven into a fabric they are periodically crimped [Fig. 1(b)]. That means that the length of the copper fiber is greater than the length of the fabric. There are several irregularities concerning the location of the fibers within the yarn as well as concerning the location of the yarns within the fabric. These variations are caused by deformability of textile material and degrees of freedom in manufacturing processes. At the level of fibers and yarns there are, e.g., variations of diameters and densities (along thread but also from thread to thread). At the level of fabrics, e.g., distance between yarns varies (Fig. 2, Table II). As textile material has viscoelastic behavior, inner tensions relieve over time and geometry may change (especially in washing treatments).

IV. MATERIAL PROPERTIES

The measured dc resistance of single copper fibers and the actual diameter of the copper wires allow to calculate the effective copper wire length compared to the textile length. For the thinner yarns (type A) the copper wire is about 7.5% longer than the corresponding textile, with a tolerance of $\pm 0.5\%$. For the thicker yarn (type C) where the copper fiber runs a larger helical path, this difference increases to about 25.5% with a tolerance of $\pm 2.0\%$.

The dielectric permittivity ϵ_r of the mixed PES-air textile structure was extracted by means of parallel plate capacitors. Two different plate sizes (10 cm $\times$ 10 cm and 4 cm $\times$ 4 cm) and eigth different plate distances (1 to 8 textile layers between

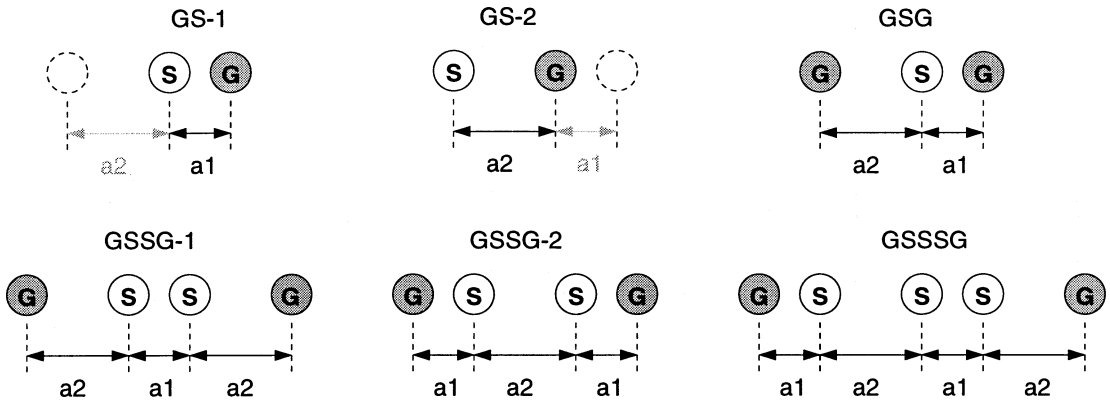

Fig. 3. Schematics of the effective transmission line configurations, G = ground, S = signal.

the plates) were used. The exact plate distance was mechanicaly measured for each configuration. All measurements were done with the yarn types B and D which have no copper fibers. The obtained results range from $\epsilon_r = 1.4$ to 1.6. These inaccurate values are due to the fact that the measured permittivity strongly depends on the ratio of polyester and air. Introducing copper fibers will also affect total permittivity as polyesterimide used for isolation coating of copper shows an $\epsilon_r \approx 3$. For any applications with strict electrical specifications it is important to keep in mind that with the given structure of fabrics permittivity is very susceptible to air humidity and moisture absorption.

V. Impedance Characterization

In this section the typical, achievable characteristic impedance of the textile transmission lines are investigated. From a design and application driven point of view, special attention is given to the accuracy of pre-determining the transmission line's characteristic impedance with regard to the fabrication tolerances listed in Table II.

A. Transmission Line Configurations

A close look into the plain weaves of our fabrics exhibits topological affinities to conventional twisted pair cables or coplanar waveguides (CPW) on printed wire boards. Based on this we chose a set of different transmission line configurations where copper fibers in X direction serve as signal line and one or more fibers on each side of the signal serve as ground reference. The transmission lines differ by the number of signal fibers S or ground fibers G. The space between the ground and the signal line is given by the textile construction and can not be modified. The attempt to skip copper fibers to increase the space would yield floating lines evoking undesired parasitic coupling effects. In effect the given textile fabrics geometry restrict the degree of freedom to the number of signal fibers S and the number of ground fibers G.

A list of all investigated configurations is given in Table III. Considering the textile geometry variations illustrated in Fig. 2 which show asymmetric yarn spaces in X direction ($a_1 < a_2$) we must differentiate two types of GS and GSSG lines. The resulting effective configurations are depicted in Fig. 3. A drawback of using the fabrics 1 and 4 (copper in XY direction) is that the unused copper wires transverse to the transmission line direction remain floating, again evoking the aforementioned coupling effects.

TABLE III
Transmission Line Configurations Used in the Experiments

Config.	Yarn type	Fabric type	Textile length
GS-1/GS-2	A	1 and 2	10 cm and 15 cm
GSG	A	1 and 2	10 cm and 15 cm
GSSG-1/GSSG-2	A	1 and 2	10 cm and 15 cm
GSSSG	A	1 and 2	10 cm and 15 cm
GS-1/2	C	4 and 5	10 cm and 15 cm
GSG	C	4 and 5	10 cm and 15 cm
GSSG-1/GSSG-2	C	4 and 5	10 cm and 15 cm
GSSSG	C	4 and 5	10 cm and 15 cm

B. TDR Measurements

Impedance measurements of the textile transmission lines were performed with time domain reflectometry (TDR) using a Tektronix CSA-803A and the IPA-501 software [10]. FR4 laminate-based interposers with patterned 50 Ω CPW solder pads on one side and SMA connectors on the other side allowed reliable connection of the textile samples with the measurement equipment (Fig. 4). The block diagram of the measurement setup is depicted in Fig. 5.

Fig. 6 summarizes the measured line impedances for the investigated transmission lines. Results for the same yarn and fabric types are connected with lines to illustrate the relation between configuration and line impedance. The qualitative results of the four configurations are comparable to coplanar waveguides on PCBs: increasing the signal line width by adding more parallel copper fibers, decreases the line impedance. But the quantitative results show that 50 Ω lines are not realizable and that even 100 Ω lines are difficult to achieve.

Comparing the results of the same fabric and the same configuration one can observe large impedance variations. However, in compliance with the textile process variations presented in Table II the thicker yarns [type C, Fig. 6(b)] have much smaller impedance variations than the thinner yarns [type A, Fig. 6(a)].

The difference of the TDR signal propagation times in the 10 cm and 15 cm samples gives an exact value of the propagation time t_d for 5 cm textile transmission lines. Using t_d and the characteristic impedance Z_0 in the (1) and (2) we obtain the

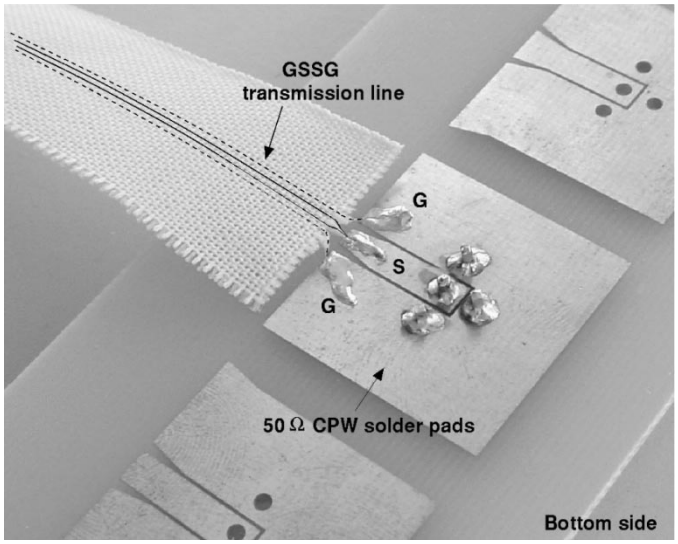

(a)

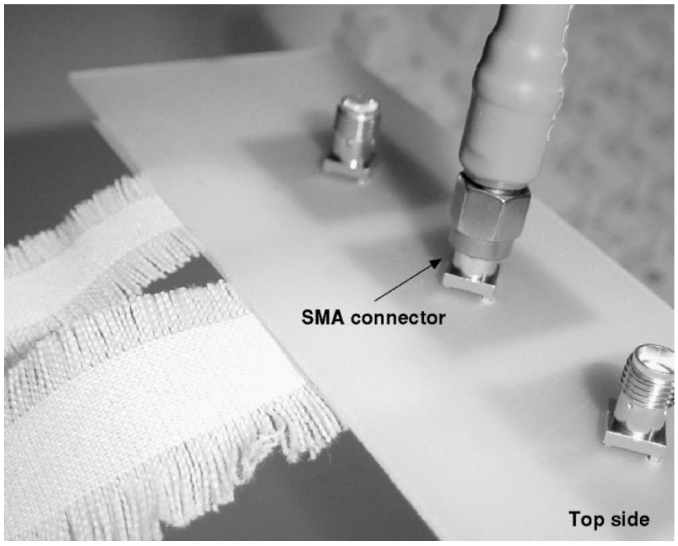

(b)

Fig. 4. Textile solder-pads as (a) 50 Ω coplanar waveguide and (b) SMA connectors.

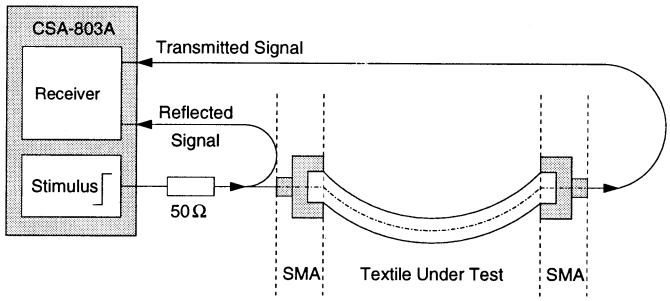

Fig. 5. Block diagram of TDR measurement setup.

transmission line equivalent parallel capacitance C_p and series inductance L_s per unit length. The extracted values for all investigated configurations are listed in Table IV. The results clearly show that the textiles with copper only in X direction have lower

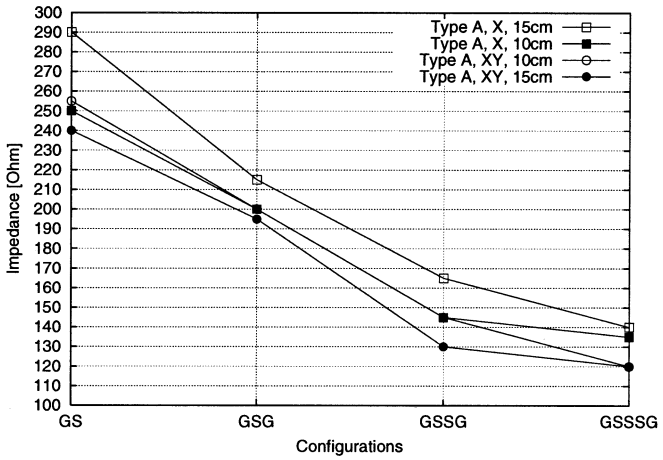

(a)

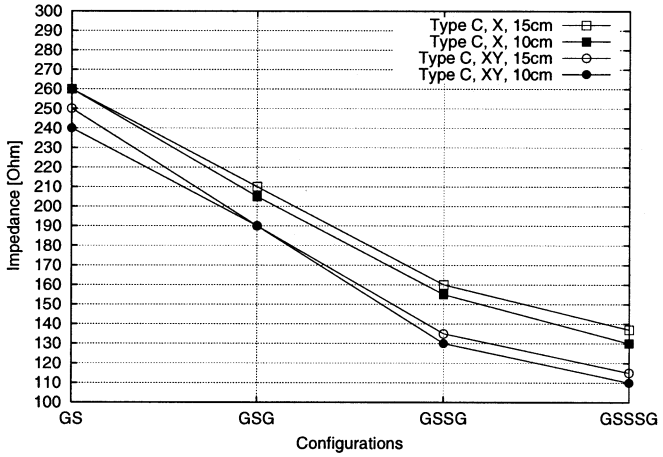

(b)

Fig. 6. Measured impedance of the different textile transmission line configurations with the yarn type A (a) and yarn type C (b).

TABLE IV
EXTRACTED EQUIVALENT PARALLEL CAPACITANCE C_p AND SERIES INDUCTANCE L_s AND MEASURED DC RESISTANCE R_{DC} FOR TEXTILES WITH CU IN X AND XY DIRECTIONS RESPECTIVELY

Yarn type and config.	C_{pX} [pF/m]	C_{pXY} [pF/m]	L_{sX} [μH/m]	L_{sXY} [μH/m]	R_{DC} [Ω/m]
A, GS	15.2	16.5	1.155	1.700	14.61
A, GSG	19.0	22.0	0.840	0.880	14.61
A, GSSG	21.2	30.7	0.544	0.602	7.31
A, GSSSG	27.0	32.5	0.546	0.468	4.84
C, GS	13.5	17.6	0.910	1.100	17.05
C, GSG	14.9	22.1	0.688	0.839	17.05
C, GSSG	22.7	33.6	0.603	0.658	8.49
C, GSSSG	25.5	40.0	0.479	0.529	5.63

capacitance and inductance and therefore provide faster signal propagation than the textiles with copper in XY direction

$$C_p = \frac{t_d}{Z_0} \tag{1}$$

$$L_s = t_d \cdot Z_0. \tag{2}$$

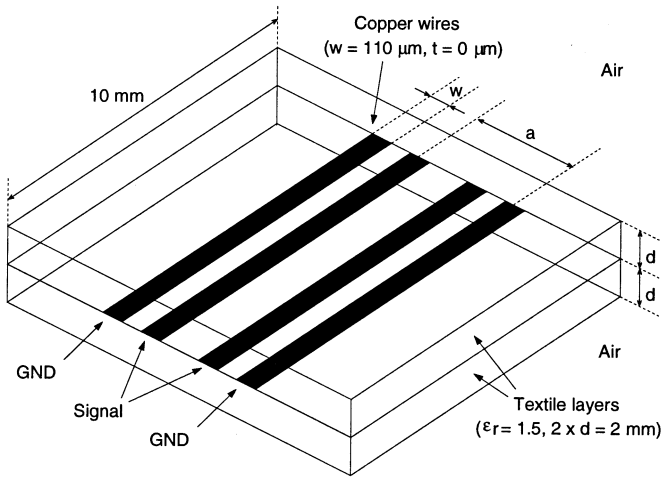

Fig. 7. Textile model for Sonnet showing a GSSG-2 configuration.

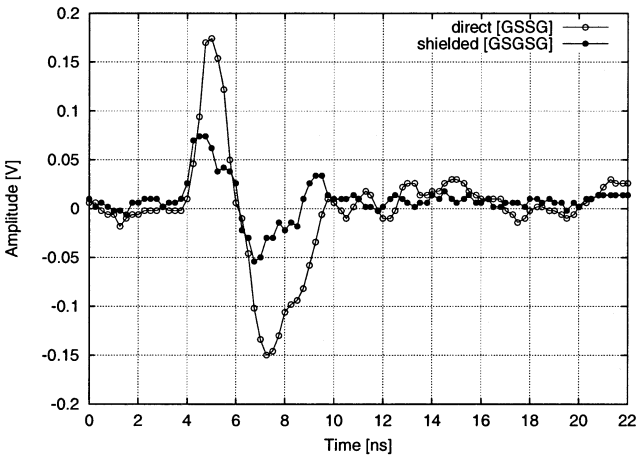

Fig. 8. Far-end crosstalk measured on 20 cm lines in GSSG and GSGSG configurations with Cu threads in X direction and matched loads.

TABLE V
SIMULATION RESULTS OF TEXTILE LINE IMPEDANCES WITH REGARD TO TEXTILE PROCESS TOLERANCES

Yarn type	Config.	Z_{nom} [Ω]	Z_{min} [Ω]	Z_{max} [Ω]
C	GS-1	263	247 (- 6.5 %)	278 (+ 5.7 %)
C	GS-2	303	293 (- 3.4 %)	313 (+ 3.3 %)
C	GSG	190	173 (- 9.8 %)	200 (+ 5.3 %)
C	GSSG-1	163	157 (- 3.8 %)	172 (+ 5.5 %)
C	GSSG-2	136	125 (- 8.8 %)	146 (+ 7.4 %)

C. Impedance Simulations

In order to get better understanding of how the textile fabrication tolerances affect the line impedance, we modeled the textile transmission lines with Sonnet EM Suite 7.0, a 2.5 dimensional EM field solver based on the method of moments (MoM) [11]. To simplify the modeling and to reduce the computation time, the woven fabric structure was regarded as homogenous material with an equivalent dielectric permittivity as previously measured in Section IV. In effect the textil model consists of two dielectric layers with a permittivity of $\epsilon_r = 1.5$ and a thickness of 2 mm each (see Fig. 7). The copper fibers are modeled as planar copper strips between the two textile layers. To compensate for the sinusoidal helical shape of the copper fiber within the yarn, the width of the copper stripes is averaged to $w = d/\pi \approx 110\ \mu\mathrm{m}$.

Table V summarizes the simulated impedances for the different configurations with yarn type C and copper in X direction, The results show good agreement with the measured values shown in Fig. 6(b). The $Z_{\min}$ and the $Z_{\max}$ values are computed using the worst case combinations of the fabric variations but with regard to the correlation between a_1 and a_2 given by $a = a_1 + a_2$. We can see that within worst case standard deviations of fabrication tolerances, impedance of two corresponding configurations GS-1 and GS-2 as well as GSSG-1 and GSSG-2 do not overlap. Hence, it is important to differentiate them as two separate configurations. For an implementation where a textile signal bus must be effectively terminated, achievable tolerance of $\pm 5\%$ to $\pm 10\%$ is accurate enough.

D. Crosstalk

Fig. 8 presents the results of far-end crosstalk for two neighboring lines in GS and GSG configurations and copper threads in X direction. The measurements were performed on two 20 cm long lines terminated in a matched load. The amplitude the aggressor signal was 2.5 Volts with a rise time of 6 ns. The ground fiber between the neighboring lines in the GSG configuration, acting as a shield, allowed to reduce the crosstalk from 7.2% in GS configuration down to 2.8%.

VI. FREQUENCY CHARACTERIZATION

To investigate the frequency characterisitcs of textile transmission lines we measured their transmission properties by means of vector network analyzer (VNA) up to 6 GHz. The textiles were connected with the network analyzer ports by means of the same FR4 interposers proposed earlier. Based on these measurements we extracted the frequency dependent attenuation constant and effective relative dielectric constant for the different textile transmission line configurations.

A. Problem Statement

Before any accurate S-parameter measurements can be performed the measurement system needs to be calibrated to remove systematic errors resulting from different reflections. In general, this is done by measuring several "known" calibration standards. Fabrication of any calibration standards on textiles is, however, impossible. Therefore, we have to rely on more complex two-step calibration procedure [12]. The first step is a standard calibration using SOLT standards for 3.5 mm SMA connectors. In this step losses, reflections and phase delays caused by the connectors, cables, transitions and switching as well as isolation errors of the VNA have been accounted for. Hence the error boxes on both sides of the DUT represent now the feeding structure consisting of SMA connector-CPW and soldered textile-CPW transitions.

The goal of the second step of the procedure is deembeding of these transitions, which have substantial influence on the measured results, especially if we measure nonmatched lines. As the

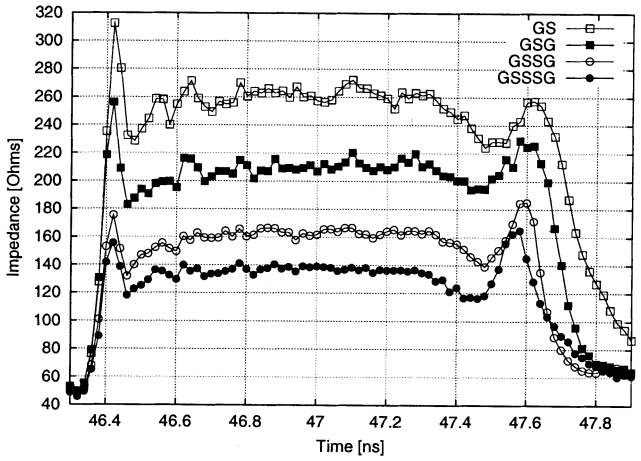

Fig. 9. Measured impedance profiles of 15 cm transmission lines with yarn type C and copper in X direction.

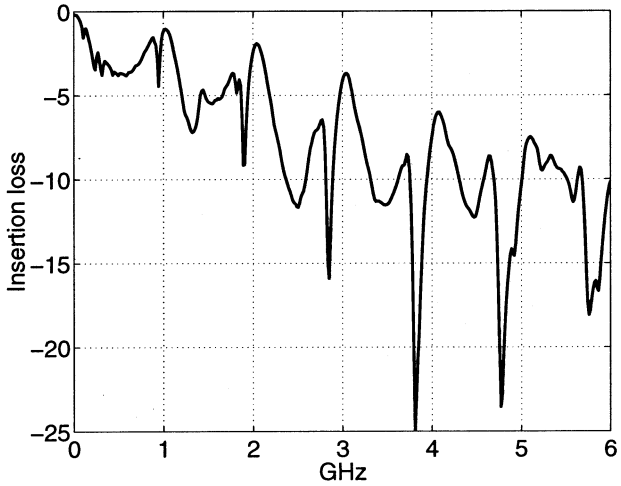

Fig. 10. Measured insertion loss in [dB] of the 10 cm GSSSG line with copper in X direction and yarn type C.

discontinuities on both sides of the DUT are equal, the measurement problem can be assumed to be symmetric, such that only one error box is to be determined. This step of the procedure depends on the measurement of two lines with different lengths.

The underlying two assumptions of this second step of the procedure are that the measured lines are uniform and that they guide only one mode. As will be shown later these two conditions can not be fulfilled perfectly. The limitations are the tolerances of the geometrical distances between the wires creating the waveguide. In effect the line can not be assumed reflectionless along the line but it continuously and stochastically changes its impedance value. Typical line impedance profiles measured by TDR for different configurations are shown in Fig. 9.

The second effect caused by the same substantial geometrical deviations is more serious and unables practically the operation of the textiles above some clearly measurable frequency point. This effect is the excitation of parasitic "odd-modes" of propagation [13]. For the proper propagation of our desired mode similar to CPW mode in CPW lines, the potentials on both GND wires should be the same along the line. The same is necessary for the wires creating the central conductor. Substantial variations of different wire lengths and distances between wires creating the transmission line are able to unequalize the phases between the appropriate lines and excite the parasitic odd-modes. In a standard CPW line the problem is avoided by use of bridges [14]. In our case this solution is not available. The appropriate GND wires and wires creating the central conductor are shorted only at the beginning and the end of the transmission line in the measured configurations in order to force the appropriate equal potentials on the lines. It creates, unfortunately, the half-wavelength resonator shorted at both line ends for the odd-modes [15]. This effect is able to forbid the transmission along the line for some discrete frequencies equal to multiple half-wavelengths of the appropriate odd-modes.

The typical measured S21 parameter for 10 cm long lines in GSSSG configuration with the thicker yarn type and copper only in warp direction prior to the second step of the extraction procedure is presented in Fig. 10. One can clearly observe some deep minima even down to -25 dB. This is the effect of the

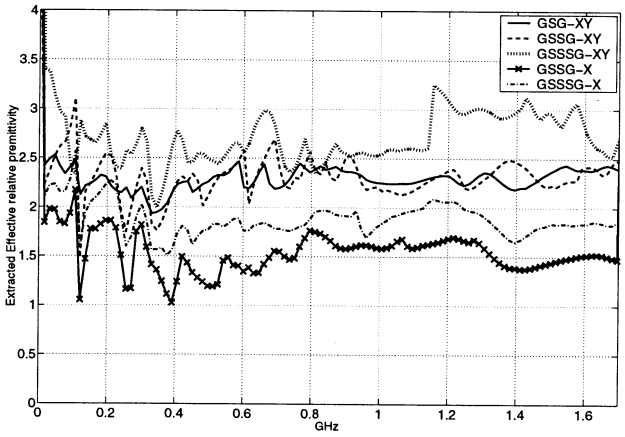

Fig. 11. Extracted effective relative permittivities of different line configurations using the thicker yarn types C.

mentioned above coupling to the odd-modes, which create resonant minima in the line transmission.

B. Effective Dielectric Constant of the Lines

Based on the presented procedure we extracted the effective dielectric constants and attenuation constants for different configurations. Fig. 11 gathers a set of the extracted values of $\epsilon_{r_{eff}}$. For every line configuration we used three different line lengths of 3, 5, and 10 cm, which allowed us to create three different line pairs and enhance the accuracy of the extracted parameters. The upper frequency limit up to which the validity of the calibration can be justified is fixed by the longest line length. This length determines the lowest resonant frequency of the odd-mode in the measured configuration. The extracted $\epsilon_{r_{eff}}$ covers the frequency range up to 1.7 GHz. These values are in the range of 1.4–1.7 for fabrics with copper in X directions and 2.3–2.5 for fabrics in XY directions.

The extracted values show some deviations in frequency because of the mentioned influences of high tolerances. These deviations cannot be interpreted as physically frequency-dependent effective dielectric constants. Nevertheless, they deliver

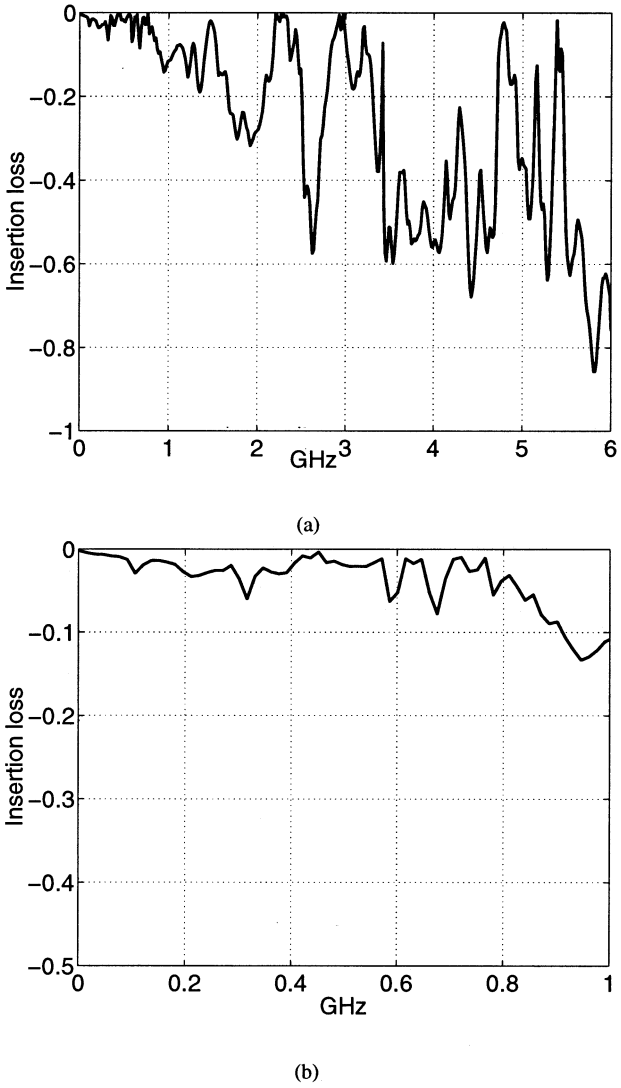

Fig. 12. Insertion loss of the GSG line in XY configuration and yarn type C in dB/cm from (a) 0 GHz to 6 GHz and (b) with more detail from 0 GHz to 1 GHz.

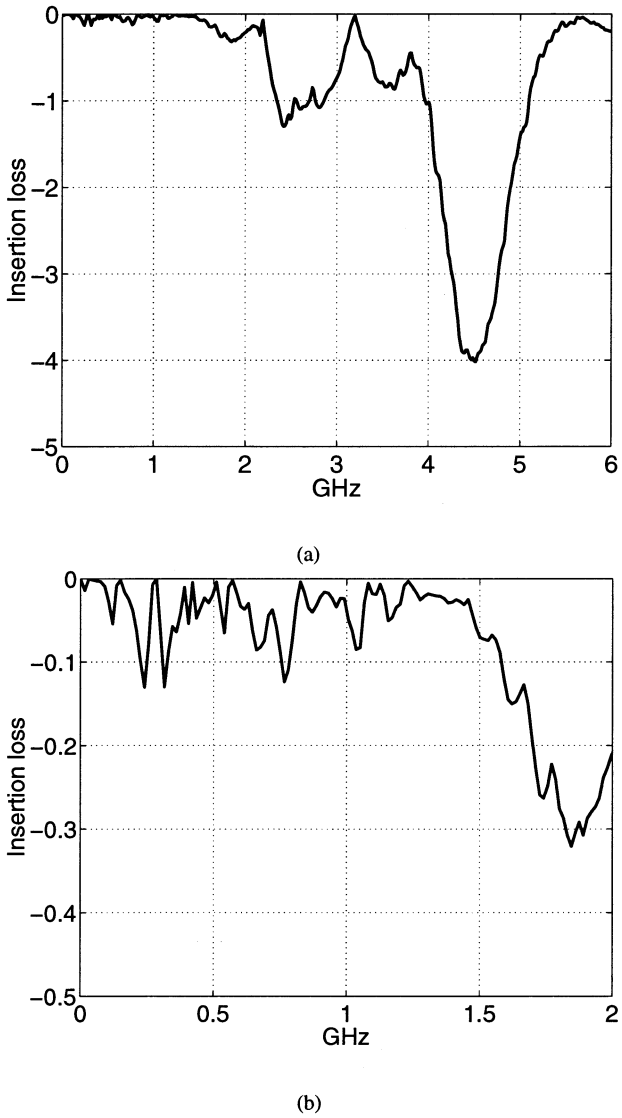

Fig. 13. Insertion loss of the GSSG line in X configuration and yarn type C in dB/cm from (a) 0 GHz to 6 GHz and (b) with more detail from 0 GHz to 2 GHz (b).

good estimation of the physical properties of the textile lines. As the extracted effective dielectric constants are very low (large amount of air) and the vertical dielectric build-up is symmetric, the propagation velocities of desired and parasitic odd-modes are very similar. As a result half-wavelength resonances for these modes can be assumed to be approximately the same.

C. Transmission Line Attenuation Constants

Typical line attenuation based on GSG lines in XY configuration (extracted based on 3 cm and 10 cm line lengths) and GSSG lines in X configuration (extracted based on 3 cm and 5 cm line lengths) are shown in Figs. 12 and 13. Two of them [see Figs. 12(b) and 13(b)] present more detailed insertion loss in the lower frequency range wherein the coupling to the odd-modes is weak and single mode propagation can be reasonably justified. One can observe that the extracted attenuation even in this frequency range shows nonmonotonical frequency behavior, which is not typical for uniform transmission lines. This is the effect of nonuniform characteristic impedance profile along the line caused by large geometrical tolerances. The frequency behavior of other tested configurations show the same dependence with the same maximum attenuation of 0.05–0.1 dB/cm in the frequency range of single mode propagation.

We can arrive at the very important conclusion that the insertion loss of the textile lines is not determined by the dielectric and ohmic losses, but by the reflections along the line in the lower frequency range and coupling to the parasitic modes at higher frequencies above half-wavelength. Although the textile wires feature very high conductivity, it plays a minor role in determining the loss factor of the lines. The XY configurations show slightly lower losses in the single mode propagation range and weaker but more irregular coupling to odd modes. This is the effect of the orthogonal wires which are able to destroy the constructive resonances of the odd modes to some extend.

Based on measured different line configurations we can conclude that the longest possible line length is equal to the half-wavelength of the lines at the maximal desired frequency of usage. It allows the lines to be 10 cm long for maximal frequency of approximately 1.2 GHz and 1 GHz for X and XY

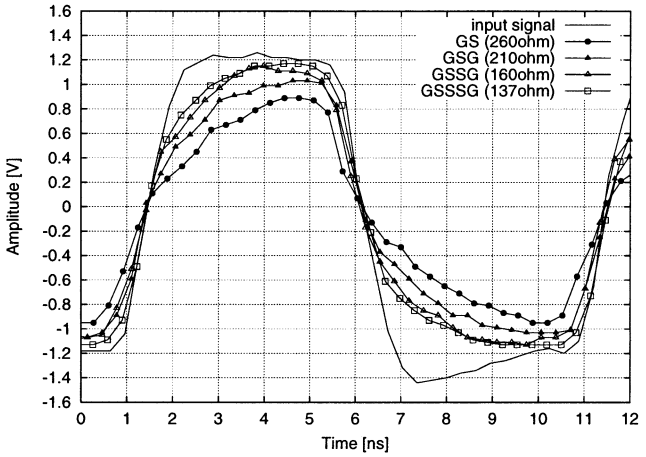

Fig. 14. 100 MHz clock signals measured through four different 20 cm long textile transmission lines.

configurations, respectively. For 100 MHz signals the allowable line lines are tenfold and are in the range of 100 cm. Fig. 14 shows a 100 MHz clock signal measured at the end of 20 cm textile transmission lines in different configurations.

VII. Conclusion

This paper presents for the first time the extensive characterization of textile transmission lines for use in wearable computing applications. The proposed textiles are fabrics with copper fibers in one or two directions and with different yarn fineness. This variety of fabrics opens a wide range of possible transmission line topologies and allows to find a configuration that fits potential target applications.

The FR4 interposer with coplanar solder pads and SMA connectors allowed reliable connection of the textile samples to the measurement equipment. TDR measurements showed that the achievable characteristic impedances lie between 120 Ω and 320 Ω. To study the influence of fabrication tolerances, the textiles were modeled with Sonnet, an EM-field simulation tool. The simulation results showed that with the given geometry variations an accuracy of $\pm 5\%$ to $\pm 10\%$ for the characteristic impedances is achievable.

High frequency network analyzer measurements were performed up to 6 GHz. The extracted frequency characteristics revealed that the dielectric and ohmic losses do not determine the line insertion loss.The loss is mainly influenced by nonuniform impedance profile along the lines up to the half-wavelength and by coupling to parasitic modes above this frequency point. This results in cut-off frequencies of 1.2 GHz and 1 GHz for 10 cm long lines in X and XY configurations, respectively. Good signal transmission for a 100 MHz clock signal was proved through 20 cm textile lines. Experiment showed also that a grounded copper fibers between two neighboring lines reduced crosstalk from 7.2% to 2.8%.

The final conclusion of this is that conductive textiles provide potentials in signal transmission in addition to EMI shielding and power supply. Transmission lines with controlled characteristic impedance and high signal integrity up to several 100 MHz enable new options of interconnect for wearable computers.

Acknowledgment

The authors would like to thank J. Bonan, A. Kuhn, and I. Ruiz, for their valuable help in the textile measurements.

References

[1] F. Gemperle *et al.*. (2002) Design for Wearability. Tech. Rep.. [Online]. Available: http://www.ices.cmu.edu/design/wearability

[2] Industrial Clothing Design. ICD+ and Wearable Electronics. Tech. Rep., Philips Electronics and Levi Strauss & Co.. [Online]. Available: http://www.design.philips.com/pressroom/pressinfo/article/icd.html

[3] J. Rantanen *et al.*, "Smart clothing prototype for the arctic environment," *Personal Ubiquitous Comp.*, pp. 3–16, June 2002.

[4] M. Coyle, "The lifeshirt system: Bringing high-tech patient monitoring from hospital to home," in *Proc. Avantex*, Frankfurt, Germany, 2002.

[5] E. R. Post, M. Orth, P. R. Russo, and N. Gershenfeld, "E-broidery: Design and fabrication of textile-based computing," *IBM Syst. J.*, vol. 39, pp. 840–860, 2000.

[6] E. J. Lind *et al.*, "A sensate liner for personnel monitoring applications," in *Acta Astronautica*. London, U.K.: Elsevier, 1998, vol. 42, pp. 3–9.

[7] S. Jung, "First results: A digital music player tailored for smart textiles," in *Proc. Avantex*, Frankfurt, Germany, 2002.

[8] X. Tao, *Smart Fibers, Fabrics and Clothing*. New York: Woodhead, 2001.

[9] H. H. Kuhn and A. D. Child, "Electrically conducting textiles," in *Handbook of Conducting Polymers*, T. A. Skotheim, R. L. Elsenbaumer, and J. R. Reynolds, Eds. New York: Marcel Dekker, 1998, pp. 993–1013.

[10] *IPA-510 Interconnect Parameter Analyzer, Reference Manual*, Tektronix, Inc., 1992.

[11] *The SONNET Suites 7.0, High Frequency Electromagnetic Software, User's Guide*, vol. 1, Sonnet Software, Inc., 2001.

[12] J. Grzyb, D. Cottet, and G. Tröster, "Systematic deembeding of the transmission line parameters on high-density substrates with probe-tip calibrations," in *Proc. 52. Electron. Comp. Technol. Conf.*, San Diego, CA, 2002, pp. 1051–1057.

[13] J. B. Knorr and K. Kuchler, "Analysis of coupled slots and coplanar strips on dielectric substrate," *IEEE Trans. Microwave Theory Tech.*, vol. 23, pp. 541–548, July 1975.

[14] E. R. Rius, J. P. Coupez, S. Toutain, C. Person, and P. Legaud, "Theoretical and experimental study of various types of compensated dielectric bridges for millimeter-wave coplanar applications," *IEEE Trans. Microwave Theory Tech.*, vol. 48, pp. 152–156, Jan. 2000.

[15] W. Lo, C. Kuang, C. Tzuang, S.-T. Peng, C. Tien, C. Chang, and J. Huang, "Resonant phenomena in conductor-backed coplanar waveguides (CBCPW's)," *IEEE Trans. Microwave Theory Tech.*, vol. 41, pp. 2099–2107, Dec. 1993.

Didier Cottet (S'99) received the M.S. degree in electrical engineering from the Swiss Federal Institute of Technology (ETH), Zürich, Switzerland, in 1997 where he is currently pursuing the Ph.D. degree in the High-Density Packaging Group, Electronics Laboratory, ETH.

His research interests include characterization and modeling of thin-film and laminate substrates for high density packaging, and technology optimization for high yield microwave and millimeter-wave system integration.

Janusz Grzyb (S'02) was born in Suwalki, Poland, on May 26, 1972. He received the M.S. degree in electrical engineering from the Technical University of Gdansk, Poland, in 1997, where he majored in microelectronics, CMOS analog design and is currently pursuing the Ph.D. degree at the High-Density Packaging Group, Electronics Laboratory, ETH, Zürich, Switzerland.

Since joining the High-Density Packaging Group in December 1998, he has been involved in MCM-based packaging and system-in-package solutions. His main interests include high frequency and microwave measurement, design, modeling and simulation of passive structures, development for MCM and related technologies, analysis and design of CMOS and BiCMOS analog and mixed integrated circuits.

Tünde Kirstein received the M.S. degree in clothing technology from the University of Applied Sciences, Hamburg, Germany, in 1996 and the Ph.D. degree from the Department of Mechanical Engineering, Dresden University of Technology, Germany, in 2001.

She was a CAD Engineer with Th. Braun (Clothing Industry), Hamburg, Germany, from 1995 to 1997, and a Lecturer for pattern construction at the Fashion Design Academy, Hamburg, from 1996 to 1997. She worked at the Institute of Textile and Clothing Technology, Dresden, Germany, during her Ph.D. studies. She joined the Wearable Computing Laboratory, Swiss Federal Institute of Technology, Zürich, Switzerland, where she is in charge of the Smart Textiles Group.

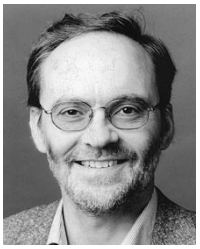

Gerhard Tröster (SM'93) received the M.S. degree from the Technical University of Karlsruhe, Germany, in 1978 and the Ph.D degree from the Technical University of Darmstadt, Germany, in 1984, both in electrical engineering.

He is a Professor and head of the Electronics Laboratory, ETH Zürich, Switzerland. During the eight years he spent at Telefunken Corporation, Germany, he was responsible for various national and international research projects focused on key components for ISDN and digital mobile phones. His field of research includes wearable computing, reconfigurable systems, signal processing, mechatronics, and electronic packaging. He authored and coauthored more than 100 articles and holds five patents. In 1997, he cofounded the spinoff u-blox ag.